Sensory Glove and Surface EMG with Suitable Conditioning Electronics for Extended Monitoring and Functional Hand Assessment

Giovanni Saggio, Giancarlo Orengo and Alberto Leggieri
Department of Electronics Engineering, Tor Vergata University, via Politecnico 1, 00133, Rome, Italy

Keywords: Sensory Glove, Surface EMG, Finger Movements.

Abstract: We propose and evaluate a new method for measuring and discriminating among flexion, extension, abduction and adduction movements of hand fingers. In particular, flex sensors allowed registering flexion-extension movements, whereas data from multi-channel surface electromyography (sEMG) electrodes allowed discriminating adduction-abduction movements of thumb, index and middle fingers. An electronic interface was designed to acquire and pre-process signals feeding a Personal Computer (PC), running indigenously made routines for data recording, visualization and storing. A novel test for repeatability and reproducibility was also proposed and successfully adopted.

1 INTRODUCTION

Sensory glove is defined as a supporting glove equipped with sensors aimed to measure hand assessment. But the hand is a masterpiece of dexterity with 27 degrees of freedom (DOFs), as determined by a widely adopted kinematic hand model (Lin et al., 2000). Therefore, usually, only a subset of DOFs is considered, and a complete 27 DOFs sensory glove is rarely realized. Those 27 DOFs include flexion/extension of the fingers' joints (i.e. the phalanges come closer/away together), abduction/adduction between fingers (i.e. the movements that bring one finger away and close from the adjacent), and rotational/translational capabilities of the wrist.

Among all, the abduction/adduction movements have been found to be the most difficult to measure. This is because flexion/extension and rotational/translational capabilities can be measured directly with a flex sensor lying on-top of the finger or of the wrist skin surfaces, but the same approach is not possible to reveal abduction/adduction capabilities.

To overcome the problem, the commonly adopted solution is to arrange a strip rectangular flex sensor upright the dorsal aspect of two adjacent fingers (Figure 1), and not between the fingers, as it would be preferable, but impracticable to avoid grasping limitations. This upright arrangement of the flex sensor can suffer from mechanical instability (since possible misplacements of the sensor during usage) and a subsequent too poor measurement accuracy, therefore here we propose to adopt surface electromyography (sEMG) sensors rather than flex ones.

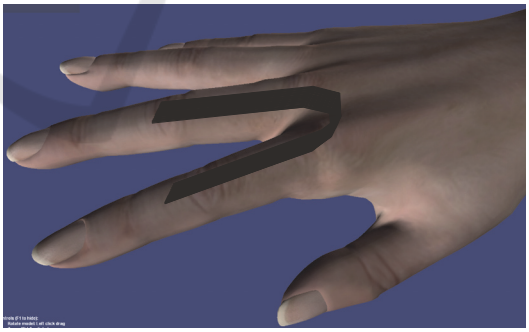

Figure 1: Strip rectangular flex sensor upright the dorsal aspect of two adjacent fingers to measure abduction/adduction angles.

In practice, we propose a combination of flex sensors and sEMG sensors for overall functional hand assessment, In fact, sEMG reveals *all* movements, so that, subtracting *flexion-extension* measures (obtained from flex sensors), we can obtain the measure of the *abduction/adduction* capabilities.

Saggio, G., Orengo, G. and Leggieri, A.
Sensory Glove and Surface EMG with Suitable Conditioning Electronics for Extended Monitoring and Functional Hand Assessment.
DOI: 10.5220/0005704702060213
In *Proceedings of the 9th International Joint Conference on Biomedical Engineering Systems and Technologies (BIOSTEC 2016) - Volume 4: BIOSIGNALS*, pages 206-213
ISBN: 978-989-758-170-0

For simplification purpose, our attention was limited to the first three finger movements, which are necessary to accomplish the most important tasks of human hand. The sEMG signals were collected by four couples of differential electrodes positioned on the right hand.

Data coming from both flex and sEMG sensors fed an Arduino microcontroller board connected to a PC. Ad-hoc PC running software was developed to represent the finger posture.

The sensory system is described in the second section of the paper, the electronic interface in the third section, the procedures used during the measurement sessions with their results in the fourth section, discussion and conclusions in the last section.

2 MEASUREMENT SYSTEM

2.1 Sensory Glove

Sensory gloves have been gaining more and more relevance in literature, even if the cost, the calibration procedure and the need of different size (to fit different hands) have limited their diffusion in clinical protocols (Gentner and Classen, 2009).

The sensory glove (Figure 2) used in this work has characteristics already reported (Saggio et al., 2012). It is equipped with 14 flex sensors (Figure 3, by Flexpoint Sensor Systems Inc. South Draper UT, USA), already reviewed in (Saggio et al., 2015), for flex-extension of all the fingers' joints, but we limited our attention to only the three sensors on the metacarpo-phalangeal joints of thumb, index and middle finger.

Figure 2: Lycra-based glove. Signals from only three flex sensor were used in this work.

Figure 3: Flex sensor from Flexpoint.

2.2 Surface EMG

Signal acquisition from sEMG sensors is rather simple, but decoding data can be challenging, because signal parameters (e.g. amplitude, frequency) are not easily linkable to subcutaneous effects. For example, the mean frequency is generally related to the muscle fatigue, even if it is not yet clear if the shift toward low frequencies is related to the speed decrease of muscular fibers (Merletti et al., 1990) rather than to the employment of slower motor units (Rau et al., 2004). The measure of muscular strength is often associated with the signal amplitude, even if it also depends on the electrode position and size with respect to the muscle, as well as the distance between electrodes. Moreover, cross-talk between different muscles adds noise to signal parameters measurement (Rau et al., 2004).

Figure 4: Location of 4 the couples of differential sEMG electrodes. The two couples of electrodes to register the index FDI, the middle TDI and the reference electrode on the wrist are shown on the leftmost photo, whereas the two couples for the thumb TA and STA on the rightmost. The cuff increases the sensor adherence to skin.

The use of sEMG to measure finger movements is mostly applied to prosthesis control by amputated people (Gentner and Classen, 2009; Riillo et al., 2014), positioning electrodes on the forearm and getting sEMG signals from extrinsic hand muscles. On the other hand, discrimination of finger movements by mean of sEMG signals associated with intrinsic muscle fatigue is still an unexplored research field, so much that even international recommendations have not yet provided instructions about electrode positioning for this kind of muscles. As a novelty, sEMG electrodes were positioned on the hand, in this case, to allow the measurement of abduction/adduction fingers' movements.

The sEMG electrodes used in this application are the "3M Red Dot" with circular shape and 60mm

diameter, their position as in Figure 4. sEMG sensor couples, for differential measures, were attached to skin surface, each along the center of the relative muscular fiber: the first dorsal interosseus (FDI, which controls the index adduction) and the third dorsal interosseus (TDI, which controls the middle adduction), on the hand span, and the short thumb abductor (STA) and the thumb adductor (TA), on the hand back.

The reference electrode on the wrist provides a common reference to the patient and to an adopted differential amplifier, to drive the isolated patient to a positive voltage respect to ground, and to reduce the 50 Hz interference from the power line. This electrode needs to be located on a neutral region as a bond, not affected by the voltages created by metabolic activity. According to SENIAM recommendations (Stegeman and Hermens, 2007), it was located on the carp pisiform bond.

3 ELECTRONIC INTERFACE

The electronics interfaced sensors with PC. It based on analog amplifiers connected to the analog inputs of an Arduino-based microcontroller device (by Smart Projects, Strambino, Torino, Italy) (Figure 5), 5V supplied via PC USB.

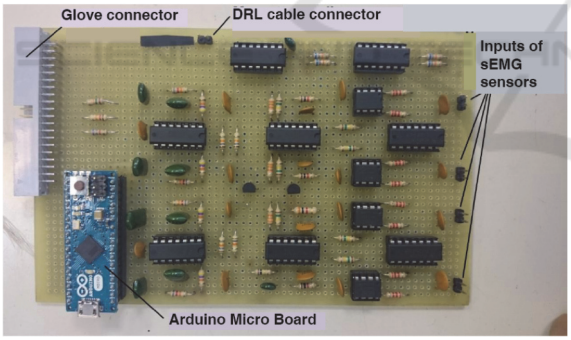

Figure 5: Stripboard of the electronic interface.

3.1 Flex Sensor Interface

Flex sensors are capable to change their resistance when bent. The output resistance of each sensor was converted into voltage values by means of voltage dividers (Figure 6), whose fixed resistances were calculated in (Saggio et al., 2012). After a buffering stage with an operational amplifier (OA), the voltage values are connected to the analog input A4, A5 and A6 of Arduino for the three fingers, respectively.

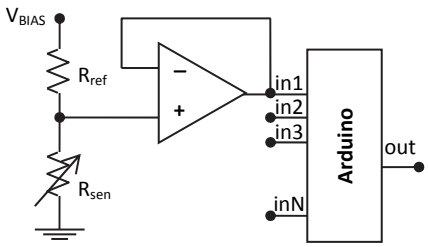

Figure 6: Schematic of the glove sensors electronic interface.

3.2 SEMG Interface

The first stage of a biopotential amplifier is an instrument differential amplifier (INA) with high CMRR. Electrical interference induced from the power line, or originating from other sources of biopotentials in more remote parts of the body, are detected simultaneously by both electrodes and were rejected by the first stage of the INA as common-mode signals. The chosen INA was the INA114 (by Burr Brown, Tucson, Arizona, USA), which features single supply mode and very high input impedance. It is dc-coupled to the electrodes via current-limiting resistors and fault current limiters.The ground path for the input bias current is therefore the body itself.

Although the INA114 has 115dB of CMRR, it decreases at a rate of 20dB/dec, becoming too low to reject strong common-mode RF signals beyond 100kHz. These random interference signals can also generate dc offset through RF rectification, which, amplified by the following gain stages, causes response errors and even saturation of solid-state devices.Therefore, the voltage gain of the INA was adjusted to 12 only, planning to yield the required gain with the following stage.

The body induced voltage from 50Hz main causes a displacement current through the patient, resulting in a common-mode voltage between the two recording electrodes and theamplifier common. This can be reduced twisting and shielding the electrode leads. Figure 7 shows a model of all the coupling capacitances and their calculated values (Neuman, 1978). Moreover, asymmetry in the two electrode impedances, due to random contact variations, transform a common-mode voltage into a differential one. Since the electrode impedance cannot be enough low, the noise signal is normally higher than the sEMG signal, which is in the range 0.1-1mV (Neuman, 1978). The common practice is to add a further electrode on the patient. But instead to connect this electrode to the amplifier reference voltage, causing a dispersion current to arise and a voltage to drop on the electrode resistance (useful to

difference the two reference voltages) (Neuman, 1978), it was connected to the driven-right-leg circuit (DRL) in a feedback loop. This is because in ECG systems it is effectively connected to the patient right leg through another electrode, whereas in sEMG systems is connected to the wrist, according to SENIAM recommendations (Stegeman and Hermens, 2007). In this way, the common-voltage is attenuated by the amplifier gain with respect to a direct connection.

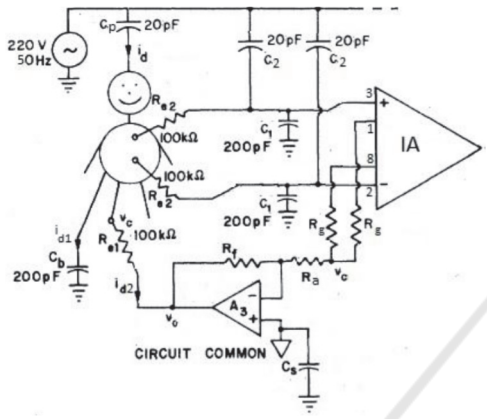

Figure 7: Circuit schematic of the parasitic coupling capacitances and the driven-right-leg circuit connecting the patient to the amplifier reference voltage to eliminate the 50 Hz noise.

In order to eliminate the so called "baseline noise" (a slow oscillation of the average signal value) which, together with movement artefacts, is considered a main noise source from electrodes, added to RF rectification and 1/f noise originated by the INA, a dc suppression circuit (Figure 8) were inserted after the INA amplifier.

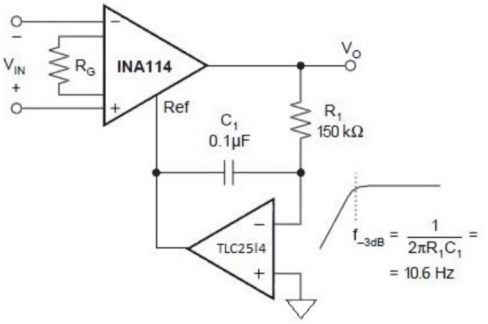

Figure 8: Output dc suppression circuit.

The integrator in the feedback loop provides ac-coupling with the following amplifier, thus changing the signal baseline with its reference voltage (Spinelli et al., 2003). The cutoff frequency was chosen, according to suggestions of International bodies (Stegeman and Hermens, 2007), equal to 10Hz.

The INA114 is followed by the second amplifying stage, a non-inverting low-pass amplifier, configured to obtain 460Hz bandwidth and a voltage gain of 180. It employs a TLC25L4ACN operational amplifier (by Texas Instrument, Texas, USA), which operated in single 5V supply mode.

Finally, a dc restoration circuit, composed of a buffered RC high-pass filter, with a cutoff frequency of 10Hz, is used to guarantee a dc level equal to 2.5V, as required by the Arduino analog-to-digital converter (ADC).

The power spectral density (PSD) of EMG signals is within 5-500Hz, but for sEMG is allowed even less bandwidth. The overall performance of the band-pass analog interface is then a 2160 voltage gain with 12Hz and 460Hz cutoff frequencies, given a 1kHz sampling frequency of the ADC.

The frequency response of the second stage amplifier, however, features only 20dB/dec of selectivity, which is too low for an anti-aliasing filter. For this reason, a Butterworth filter was realized, based on a second order Sallen-Key cell with 40dB/dec attenuation (Figure 9). The cutoff frequency of 150Hz was to provide 20dB attenuation @ 470Hz (a higher degree filter would provide more attenuation but less smooth time response and unacceptable transients). The full schematic of the sEMG interface is shown in Figure 10.

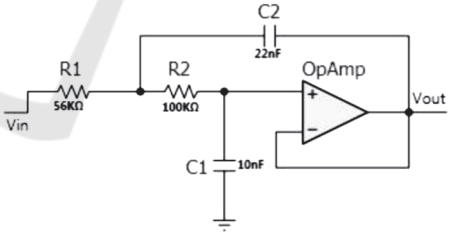

Figure 9: Second order anti-aliasing Butterworth filter.

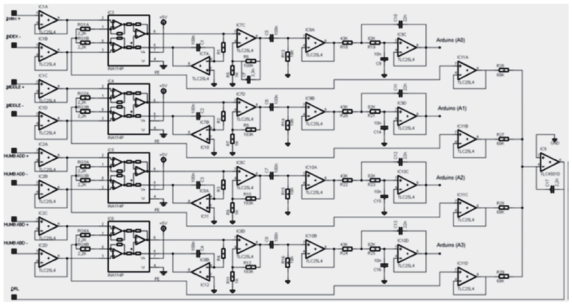

Figure 10: Schematic of the 4-channel electronic interface for sEMG sensors.

3.3 Digital Interface

For signal conditioning, signal dc offset was set to 2.5V, which was also chosen as the patient reference voltage, given through the reference electrode. Therefore, this voltage represents the signal ground for the circuit.

Data were conditioned by an Arduino Micro board, based on an ATmega32u4 (by Atmel Corporation, San Josè, California, USA) microcontroller device.

In order to maximize the communication speed, data were stored in a 14 byte register (2 byte each 10-bit value), and send as binary data (Serial.write() command) without ASCII conversion (Serial.print() command) every one millisecond. Arduino Micro sends its data to the computer at a speed of 400kbps.

A Matlab application was developed to record and save the data in text files, setting the baud rate to 460800 bps, the buffer length, and specifying the data length (two bytes always positive) according to the script *uint16*. The code reads 100 records at the same time, each corresponding to a 10-bit digitalized voltage printed by Arduino on the serial port, and plots them in real time. The effective voltage is obtained from its digital value N from the equation $V=5N/1023$.

Further noise was detected on the resulting signal, which was filtered through a digital band-pass Butterworth filter, with a low cutoff frequency of 20Hz, and a high cutoff frequency of 495Hz, to attenuate the high frequency harmonics generated by the sampling process. The root mean square (RMS) value is then calculated on a window of 300 samples, shifting it by 75 samples each time.

4 sEMG MEASUREMENTS

In this section data registration and modeling of sEMG static measurements of abduction/adduction posture of the thumb, index and middle fingers are presented. Data were acquired from six able-bodied subjects, 3 male (M1,M2,M3) and 3 female (F1,F2,F3), five right-hand and one left-hand, each one using his/her dominant hand.

Measurement results from different subjects show a remarkable spread. Then assessment of sEMG activity needs to be each time calibrated on the subject. A personal characterization session was defined to this purpose, where the number of measurements were reduced as much as a provided tolerance is still guaranteed by the extracted model. At this point, the measurement session related to a particular task can be start.

4.1 Wise Test

Since the novelty of our approach, a new test to evaluate the repeatability and reproducibility of finger abduction/adduction movement assessment was created. It was based on the Wise test provided for flexion/extension measurement, used to evaluate the performance of the electronic gloves (Gentner and Classen, 2009; Dipietro et al., 2003).

It consisted in placing and re-placing the hand in known postures always with the glove and sEMG sensors donned, to evaluate measurement repeatability, and placing and re-placing the hand in known postures after donning and doffing the sensors, to evaluate the measurement reproducibility. In particular, the postures were a) flat hand with closed fingers (starting posture), b) flat hand with 20° thumb abduction, c) flat hand with 10° index abduction, d) flat hand with 10° middle abduction.

A further posture with the maximal voluntary contraction (MVC) is also drawn for each finger. The three abduction angles to be measured are far from the MVC reported in Table 1, then easily performed and repeated by each subject (Merletti et al., 1990), which had to open the fingers up to the chosen abduction angle and hold it for 2s, during which the sEMG signals are registered, then back to the starting posture, where the resting sEMG signals are recorded. This task was repeated 10 times with a rest interval of 10s between them. After this sequence, the subject was asked to perform abduction to the MVC for each finger, in order to identify a regression of the sEMG signal intensity against the abduction angle with three points, that is 0°, 10° and MVC. Finally a data block is created. This procedure is repeated 10 times with a resting period of 3min each time. In order to evaluate the repeatability, the same sEMG sensors were used to measure the two positions (0°-10°), performing task A-C, whereas the sEMG sensor were changed after each sequence to evaluate the reproducibility (task B-D).

Table 1: MCV values for index and middle abduction.

subject	M1	M2	M3	F1	F2	F3
index	25	25	30	30	15	20
middle	25	25	30	30	25	20

Each block is composed of 2000 elements, obtained from the RMS value of the signal samples registered

during the resting intervals. The first 25 samples were eliminated, because affected by movement artefacts, and the RMS value is calculated on the next 150 samples.

From the total mean $\bar{x}_{tot}$ of the 10 blocks of the test, and the standard deviation σ of all the blocks of measurements, the uncertainty of measurements can be expressed as $\bar{x}_{tot} \pm SD/2$, from which the test results were measured through the *normalized standard deviation* (percentage) $\bar{\sigma}$, that is the ratio between standard deviation and the total mean value. It ranges from 8.28%, corresponding to $10° \pm 0.414°$ (FDI-testA-F2), to 21.1% (FDI-testB-F1), corresponding $10° \pm 1.06°$. The results for the middle finger are $\pm 0.6°$ (TDI-testA) and $\pm 1.15°$ (TDI-testB). Results for test B (0° abduction) without sEMG signals are generally worst, because the baseline measurement is more affected by noise.

4.2 Regression Models

To characterize the abduction/adduction angles against the RMS value of the sEMG signal, more data points are needed than two used for the Wise test. For this purpose, a hinge with a fixed and a mobile arm was inserted between the couple of fingers under measurement, in order to provide a finger posture with the right abduction angles, ranging from 0° to the MVC, with a 5° step. The mobile arm of the hinge was moved by a Trinamic step motor driven by a Labview interface. Although the hinge could be seen as a constrain, the subject was asked to provide the same strength as if the hinge would not be used.

Although regression models should allow obtaining the abduction/adduction angle from the measured voltage, as independent variable, it would be hard to yield models from not always univocal relations. On the other hand, if the independent variable is the angle step, as in this case, good fitting results can be yield. The inverse function can be obtained through a numerical algorithm, because the regression functions are hardly ever invertible.

Different regression models were tried to interpolate the available data, either polynomial models from the linear one to fifth degree, and the monomial/binomial exponential models, which are described in Equations (1) and (2). Each model was statistically evaluated by mean of the R^2 coefficient, which computes the correlation degree between data and model points.

$$y = ae^{bx} \quad (1)$$

$$y = ae^{bx} + ce^{dx} \quad (2)$$

4.2.1 Index/Middle Abduction/Adduction

The measurement of the sEMG voltage, representing the muscle fatigue, against the imposed angle is reported in Figures 11 and 12 for the FDI (index) and the TDI (middle), respectively, here limited to subject M1 for sake of brevity.

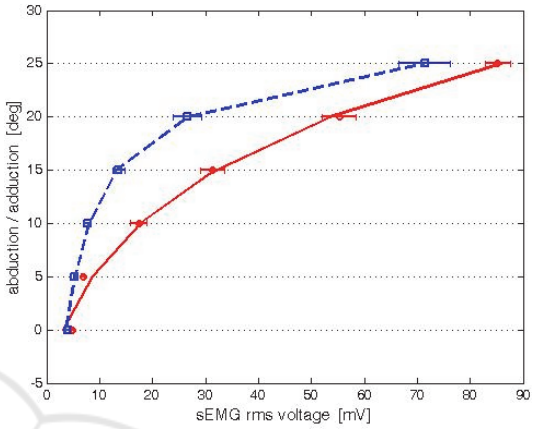

Figure 11: FDI sEMG assessment for subject M1 of middle abduction (red circle) and adduction (blu square) with standard deviation segments, superimposed to the corresponding binomial exponential regression models (continuous for abduction and dashed for adduction).

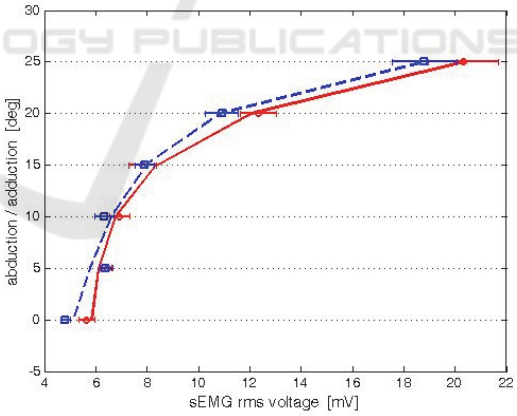

Figure 12: TDI sEMG assessment for subject M1 of middle abduction (red circle) and adduction (blu square) with standard deviation segments, superimposed to the corresponding binomial exponential regression models (continuous for abduction and dashed for adduction).

The measurement of the abduction and the adduction movements are represented with different symbols. The difference between the muscle fatigues in the two phases is marked more for the FDI than TDI in all subjects. Figures also report the measure

of the standard deviation, whose results are summarized in Table 2, as mean value between the six subjects, and compared with the corresponding ones from the test.

Taking into account the regression R^2 parameter reported in Table 3, the linear model demonstrated to be not suitable to represent the voltage/angle relation. The performance of the binomial exponential regression model is also plotted in each figure.

Table 2: Comparison of the mean normalized standard deviation between subjects.

	FDI	TDI
Wise test	10.88%	11.17%
Hinge meas	10.87%	10.56%

Table 3: Comparison of R^2 correlation coefficient for five polynomial and two exponential regression models of index FDI and middle TDI measurements.

	FDI		TDI	
model	abduct	adduct	abduct	adduct
1st	0.91	0.71	0.76	0.79
2nd	1	0.95	0.96	0.95
3rd	1	0.99	1	1
4th	1	1	1	1
5th	1	1	1	1
mon.	0.99	0.99	0.90	0.92
bin.	0.99	0.99	0.99	0.99

4.2.2 Thumb Abductor/Adductor

The same procedure was used to measure the radial abduction/adduction of the thumb, except for, this time, both the thumb abductor (TA) and the short thumb adductor (STA) operate an abduction movement when their intensity is growing, and an adduction movement when is decreasing.

Table 4: Comparison of R^2 correlation coefficient for five polynomial and two exponential regression models of TA and STA adduction/abduction measurements.

	TA		STA	
model	abduct	adduct	abduct	adduct
1st	0.76	0.62	0.65	0.77
2nd	0.98	0.94	0.98	0.99
3rd	1	0.99	1	1
4th	1	0.99	1	1
5th	1	1	1	1
mon.	0.98	0.91	0.87	0.96
bin.	1	0.98	1	1

Measurement results and the binomial exponential regression models are reported in Figures 13 and 14, whereas the R^2 results of each model are reported in Table 4.

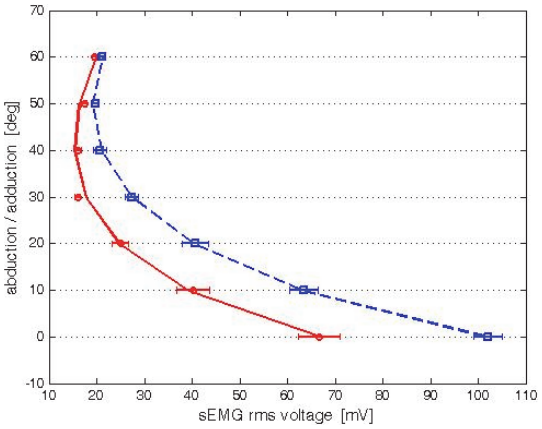

Figure 13: TA sEMG assessment for subject M1 of abduction (red circle) and adduction (blu square) with standard deviation segments, superimposed to the corresponding binomial exponential regression models (continuous for abduction and dashed for adduction).

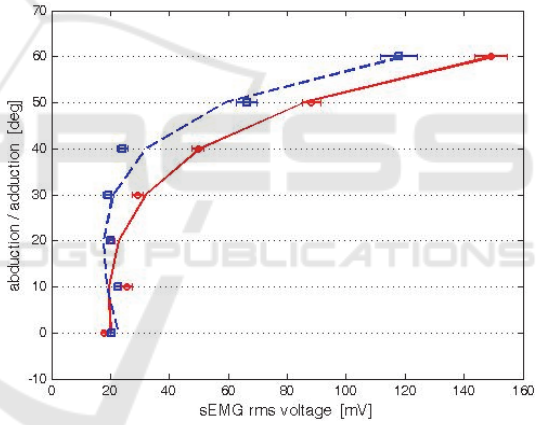

Figure 14: STA sEMG assessment for subject M1 of abduction (red circle) and adduction (blu square) with standard deviation segments, superimposed to the corresponding binomial exponential regression models (continuous for abduction and dashed for adduction).

In this case, it is worth noting that there is ambiguity for high abduction/adduction angles for TA and low angles for STA, suggesting that the two measurements can be complementary within the same algorithm, provided to discriminate the thumb position.

4.3 Finger Position Recognition

SEMG measurements of abduction/adduction were integrated with those of flexion/extension from flex sensors, to provide a complete identification of the

finger position. Bend angles were obtained through a linear relation with the sensor response.

The intrinsic muscles involved in the abduction movements, however, are activated also during flexion/extension movements. In order to discriminate the sEMG signal corresponding to the abduction movement, the flex sensor response was used.

Taking into account that for the index and middle abduction the maximum amplitude is obtained without any finger flexion, on one hand, and the abduction angle is constrained to zero at the maximum finger flexion, on the other, it was defined a bend coefficient α to modulate the sMEG response, according to equations (3) and (4)

$$\alpha = \left(90° - \vartheta_{flex}\right)/90° \quad (3)$$

$$\vartheta_{abd\_eff} = \alpha \cdot \vartheta_{abd\_reg} \quad (4)$$

On the contrary, the flexion and abduction movements of the thumb are independent, and can be actuated simultaneously.

5 CONCLUSIONS

In this paper the combination of flex and sEMG sensors was considered to measure abduction/adduction capabilities of the first three fingers. The sEMG signals were integrated with information taken by flex sensor, to discriminate the muscle fatigue devoted to abduction/adduction movements from that devoted to flexions/extensions. As a novelty, sEMG electrodes positioned on the hand allowed a measurement of abduction/adduction fingers' movements.

Data from both sensors' type fed an ad-hoc realized circuitry based on an Arduino microcontroller. PC running software was developed to represent the finger posture with bar plots.

A problem which is still to overcome is the personal characterization of the system, which has to be accomplished by each subject before to start the measurement session. Moreover, in the case of thumb position recognition, both TA and STA measurements need to be simultaneously available to extract the actual abduction/adduction angle.

Future developments can be the reduction of cross-talk between sEMG sensors, the integration of the thumb opposition measurement, and the dynamic posture recognition other than the static ones.

ACKNOWLEDGEMENTS

This paper was partially based on a work supported by the Italian Space Agency (ASI), contract #2013-081-R0, for which we would like to thank Prof. Mariano Bizzarri, Dr. Simona Zoffoli and Dr. Francesca Ferranti.

REFERENCES

Dipietro L., Sabatini A., Dario P., 2003. Evaluation of an instrumented glove for hand-movement acquisition. *Journal of Rehabilitation Research and Development*, N. 2, 181-191.

Gentner R., Classen J., 2009. Development and evaluation of a low-cost sensor glove for assessment of human finger movements in neurophysiological settings. *J. Neurosci. Methods*, 178, 138-147.

Lin J., Wu Y. and Huang T. S., 2000. Modeling the constraints of human hand motion. *IEEE Workshop on Human Motion*, 121-126.

Merletti R., Knaflitz M., & De Luca C. J., 1990. Myoelectric manifestations of fatigue in voluntary and electrically elicited contractions. *J. Appl. Physiol.*, 69(5), 1810-1820.

Neuman M. R., 1978. Biopotential amplifiers", *Medical Instrumentation: Application and Design*. Webster J. G., Ed. Boston, MA: Houghton Mifflin.

Rau G., Schulte E., & Disselhorst-Klug C., 2004. From cell to movement: to what answers does EMG really contribute?. *Journal of Electromyography and Kinesiology*, 14(5), 611-617.

Riillo F., Quitadamo L. R., Cavrini F., Gruppioni E., Pinto C.A., Pastò N.C., Sbernini L., Albero L., Saggio G. 2014. Optimization of EMG-based hand gesture recognition: supervised vs. unsupervised data preprocessing on healthy subjects and transradial amputees. *Biomedical Signal Processing and Control*, Vol. 14, 117-125.

Saggio G., Lagati A., Orengo G., 2012. Wireless Sensory Glove System developed for advanced Human Computer Interface. *International Journal of Information Science*, 2(5), 54-59.

Saggio G., Riillo F., Sbernini L., Quitadamo LR, 2015. Resistive flex sensors: a survey. Smart Materials and Structures, Volume 25, Number 1, pp. 1-30.

Spinelli E. M., Pallàs-Areny R., & Mayosky M. A., 2003. AC-coupled front-end for biopotential measurements. *IEEE Trans. on Biomedical Engineering*, 50(3), 391-395.

Stegeman D., & Hermens H., 2007. Standards for surface electromyography: The European project ″Surface EMG for non-invasive assessment of muscles (SENIAM).